

Model to Study the Effect of Composition of Seawater on the Corrosion Rate of Mild Steel and Stainless Steel

Subir Paul

(Submitted December 5, 2009; in revised form April 7, 2010)

Mild steel and 304 stainless steel are the versatile materials of construction for various structures in ocean water, whose composition varies widely in the vast global marine environment. The major parameters influencing the rate are salinity, sulfate, bicarbonates, pH, and temperature and dissolved oxygen. Prediction of the rate of degradation is a challenging task for design and corrosion engineers for existing as well as new structures to be constructed. Endeavors have been made to model the corrosion rate of mild steel and 304 stainless steel as function of five parameters, namely chloride, sulfate, dissolved oxygen, pH, and temperature, based on laboratory experimental data. The number of experimentations and compositions of experimental artificial seawater were based on 2^k factorial design of experiment. The model was validated with additional generated experimental data as well as real field study from the literature. Three-dimensional mappings of corrosion behavior of mild steel and stainless steel reveal that the effects of these parameters are interrelated and influenced by one another.

Keywords carbon steel, corrosion testing, modeling processes, stainless steel

1. Introduction

The geographical variation in the corrosivity of natural seawater results from the variation of salinity, temperature, dissolved oxygen concentration, and the presence of various other salts. Chloride ion (Cl^-) has strong influence on the corrosivity of structural steel. The chloride (Cl^-) concentration of seawater varies from about 5.8 to about 24 g/kg, sulfate (SO_4^{2-}) from 0.8 to 3.4 g/kg, and the bicarbonate (HCO_3^-) from 0.01 to 0.2 g/kg (Ref 1) across the different ocean and seawater. Increase of temperature and dissolved oxygen [O] concentration is known to aggravate the degradation rate of the structural material. Though the pH of seawater is in the range of neutral to slightly alkaline, local acidity may be developed due to corrosion products as well as crude petroleum products, lowering pH to around pH 4. It is interesting to find the effect of sulfate (SO_4^{2-}) which also influences the corrosion rate of steel.

There had been some laboratory studies (Ref 2) and fields' studies (Ref 3-5) of corrosion of mild steel in seawater. Melchers et al. conducted field tests at Swansea Public Wharf and at Pelican Marina (Ref 3) and had reported 0.13 mm/day as the rate of material loss at Swansea Public Wharf. Various models are found in the literature to predict corrosion rate and other corrosion properties from the field test data. Sridhar et al. (Ref 6) developed a model to predict the localized corrosion of steel in seawater. They predicted the repassivation potential and corrosion potential of stainless steel. Temperature is also known

to have a strong effect on marine corrosion of carbon steel. Melchers and Jeffrey (Ref 7) built a model on the corrosion rate of mild steel from the field data of salinity, pH, sulfate concentration, and dissolved oxygen at different geographical locations. Free and coworkers (Ref 8, 9) developed a mathematical model based on thermodynamic, kinetics, and mass transport equations to predict corrosion of steel in aqueous media with the variations of solution compositions.

In this study, endeavors have been made to develop a model to simulate the corrosion rate for a given geographical location in an ocean from laboratory generated data and study a comparative corrosion behavior of low carbon structural steel and 304 stainless steel, with variation of constituents' salts, temperature, pH, and dissolved oxygen. The full range of constituents' salts, temperature, pH, and dissolved oxygen were selected for series of experimentations based on 2^k factorial design of experiment (Ref 10).

2. Experimental Procedure

Rectangular samples of $1 \times 2 \text{ cm}^2$ were cut from 304 stainless steel and low carbon steel. They were ground carefully in order to make the edges blunt and to give a near rectangular cross section. The samples were then further ground by belt drive and polished up to 3/0 emery paper. Polishing provides a uniform surface, removes the surface defects that could serve as pit sites. Following this, the samples were washed with acetone and then left to be air-dried. The samples were observed with low magnification microscope to observe whether there was any pit or deep scratch on the polished surface. If any deep scratch or pits were observed, the samples were further polished.

Fresh solutions were prepared before each experiment, using KCl , CaCl_2 , NaHCO_3 , and MgSO_4 salts in double distilled water with various combinations of concentration of chloride, sulfate, dissolved oxygen contents, temperature, and pH for the series of experiments in accordance with the factorial design of

Subir Paul, Department of Metallurgical and Material Engineering, Jadavpur University, Kolkata 700032, India. Contact e-mail: spaulxx@ymail.com

experiment (See Table 1), and some more experiments were conducted at other different combinations for validation of the model (See also appendix Table A1).

Standard corrosion cell was used to perform the electrochemical potentiostatic polarization tests on standard flat metal specimens. Polarization experiments were carried out as per ASTM standard methods (Ref 10-14), using Gamry Potentiostat. Corrosion rates were determined by Tafel's extrapolation and linear polarization method.

3. Factorial Design of Experiment

Factorial experiment design (Ref 15) is a systematic method for formulating the steps needed to successfully implement the experiments that investigate the effects of two or more factors or input parameters on the output response with a minimal number of observations. A two level factorial design of experiment means two levels of each factor will be studied at once. If there are k factors or input variables influencing the output, minimum 2^k no of experiments are needed to evaluate the factors affecting the process or output. Each factor will have two levels, a "high" and "low" level. In this investigation, five factors have been selected with two level factorial design of experiment, as illustrated in Table 1.

Let Z_j^{\max} = upper limit of the variable j and Z_j^{\min} = lower limit of the variable j

$$Z_j^0 = \left(Z_j^{\max} + Z_j^{\min} \right) / 2; \quad (\text{Eq } 1)$$

$$\Delta Z_j = \left(Z_j^{\max} - Z_j^{\min} \right) / 2, \quad (\text{Eq } 2)$$

where Z_j^0 is the center point of design or basic level and ΔZ_j is the interval of variation on the Z_j axis. It is usual to change the coordinate system of $Z_1, Z_2 \dots Z_j$ to a new dimensionless system of coordinates of $X_1, X_2, \dots X_j$ such that dimensionless variable X_j is related by Z_j by the following equation

$$X_j = \left(Z_j + Z_j^0 \right) / \Delta Z_j, \quad (\text{Eq } 3)$$

where $j = 1, 2, \dots k; k = 5$.

Using this factorial design, the regression equation is given as follows:

$$Y = f(b_j, X_j) = b_0 + b_1 X_1 + b_2 X_2 + \dots + b_{12} X_1 X_2 + \dots + b_{123} X_1 X_2 X_3 + \dots + b_{12345} X_1 X_2 X_3 X_4 X_5, \quad (\text{Eq } 4)$$

where b is the interaction coefficient, and X is dimensionless variable. The significance of the interaction coefficients is

Table 1 Composition of different variables in 2^5 factorial design of experiments

Variables	Reagents	Upper limit Z_j^{\max}	Lower limit Z_j^{\min}	Average for Z_j^0
X1	Chloride	24 g/L	15 g/L	19.5 gm/L
X2	Sulfate	3.4 g/L	0.8 g/L	2.1 gm/L
X3	pH	8	4	6
X4	Temperature	40 °C	10 °C	25 °C
X5	Dissolved oxygen	10 ppm	2 ppm	6 ppm

tested by Student t distribution with 95% confidence limit. The regression equation is adequately fit by F distribution test with 99% confidence limit. The model was developed based on regression equation. The assumptions are, that the model is valid in seawater within certain range of compositions of the constituents given by Table 1, under near stagnant and at constant temperature. A Software was built to predict the corrosion rate with a given composition of seawater and to generate 3D corrosion mapping, using Matlab.

4. Results and Discussions

The model to predict the corrosion rate of stainless with variation of Cl, pH, and SO₄ are given as

$$I_{\text{corr}} = 1.186 + 0.659 * ((Cl - 19.5) / 4.5) + 0.189 * ((SO_4 - 2.1) / 1.3) + 0.354 * ((pH - 6) / 2) + 0.213 * ((SO_4 - 2.1) / 1.3) * ((pH - 6) / 2) + 0.219 * ((Cl - 19.5) / 4.5) * ((SO_4 - 2.1) / 1.3) * ((pH - 6) / 2)$$

and that for mild steel with variations of five parameters Cl, pH, SO₄, [O], and T are given as

$$I_{\text{corr}} = 64.225 + 19.82 * ((Cl - 19.5) / 4.5) + 2.87 * ((pH - 6) / 2) - 7.42 * ((SO_4 - 2.1) / 1.3) * ((pH - 6) / 2) - 4.17 * ((Cl - 19.5) / 4.5) * ((pH - 6) / 2) - 9.32 * ((Cl - 19.5) / 4.5) * ((SO_4 - 2.1) / 1.3) * ((pH - 6) / 2) + 36.35 * ((Cl - 19.5) / 4.5) + 54.06 * ((T - 25) / 15) + 41.92 * (([O] - 6) / 4) + 41.79 * ((Cl - 19.5) / 4.5) * ((T - 25) / 15) + 37.86 * ((T - 25) / 15) * (([O] - 6) / 4) + 22.34 * ((Cl - 19.5) / 4.5) * (([O] - 6) / 4) + 23.30 * ((Cl - 19.5) / 4.5) * ((T - 25) / 15) * (([O] - 6) / 2)$$

5. Validation of the Model

Besides series of experiments based on factorial design to develop the model, some additional experiments were

Table 2 Experimental conditions for validation of the model for 304 stainless steel

Expt. no	Cl, g/L	SO ₄ , g/L	pH
1	15	3.92	4
2	20.4	0.8	4
3	24	3.4	4
4	24	3.4	4.8
5	18.6	3.4	8
6	24	3.4	5.6
7	24	3.4	6.4

conducted to validate the model, at various random combinations of Cl⁻, SO₄²⁻, pH, temperature, and [O]. The experimental conditions for different experiment number are given in Table 2 and 3 for 304 steel and mild steel, respectively. The comparisons of experimental I_{corr} with the I_{corr} values computed from the model have been illustrated for stainless steel in Fig. 1 and mild steel in Fig. 2. It is seen that the computed values come out close to experimental values and the percentage errors are within $\pm 10\%$.

Table 3 Experimental conditions for validation of the model for mild steel

Artificial seawater with KCl, CaCl ₂ , NaHCO ₃ and MgSO ₄ salts with various combinations of concentration of chloride, sulfate, dissolved oxygen contents, temperature, and pH					
Expt. no.	Cl, g/L	SO ₄ , g/L	pH	Temperature, °C	[O], ppm
1	15	2.36	4	25	6
2	15	0.8	5.6	25	6
3	16.8	3.4	8	25	6
4	22.2	0.8	4	25	6
5	24	0.8	4	25	6
6	24	3.4	6.4	25	6
7	25.8	0.8	4	25	6
8	24	1.32	8	25	6
9	24	3.4	5.6	25	6
10	24	0.8	8	25	6
11	24	0.28	8	25	6
12	24	2.1	8	40	3.6
13	16.8	2.1	8	40	10
14	24	2.1	8	22	10
15	24	2.1	8	40	5.2
16	18.6	2.1	8	40	10
17	24	2.1	8	28	10
18	24	2.1	8	40	6.8
19	20.4	2.1	8	40	10
20	24	2.1	8	34	10
21	24	2.1	8	40	8.4
22	22.2	2.1	8	40	10
23	24	2.1	8	40	10

6. Prediction of Corrosion Rate

Attempts have been made to predict the corrosion rate of real structures submerged in seawater at any geographical location, from the model.

It is found from the literature (Ref 3, 7) that the corrosion rate of low carbon structural steel at a specific location in the ocean (Swansea Wharf), with average composition of 29.8–34.9 g salinity, 2.4 g/L SO₄²⁻, and pH 8 is 0.471 mm/year.

With above constituents in seawater, the corrosion rate comes out from the model, is 0.435 mm/year. It is interesting to find that the computed corrosion rate is very close to one determined in the real situation.

7. Corrosion Behavior of Stainless and Mild Steel

Effects of various corrosion influencing parameters on corrosion behavior of the 304 steel and the mild steels, based on the derived model, have been discussed in the following sections.

Figure 3 depicts 3D surface of corrosion of 304 stainless steel in seawater with variation of chloride and pH. It is seen as expected, the corrosion rate increases with the chloride

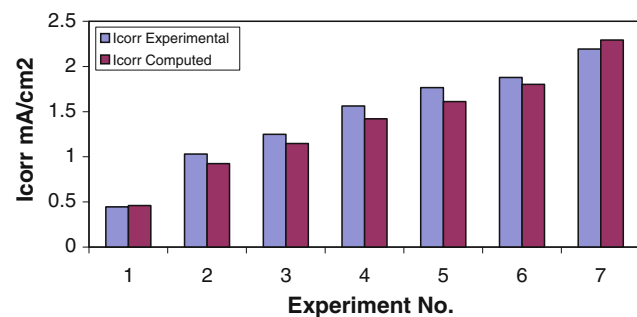


Fig. 1 Comparison of corrosion rates between experimental and computed results from the model for 304 steel in artificial seawater at various combinations variables as given in Table 2

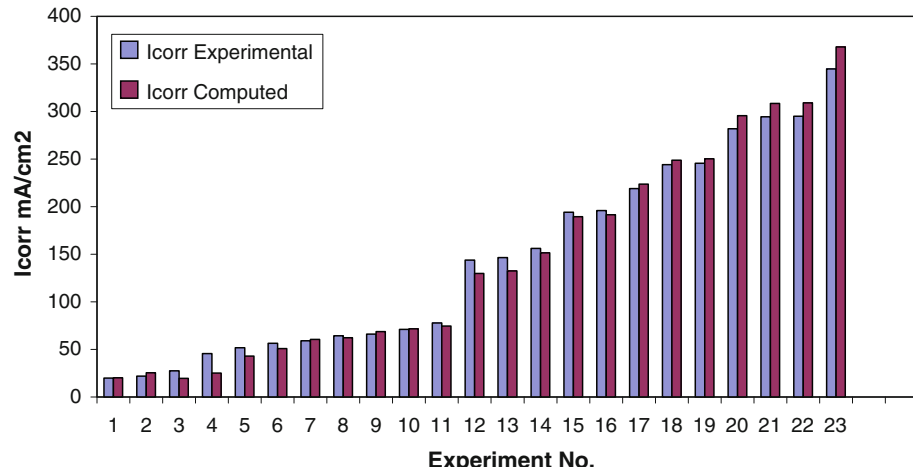


Fig. 2 Comparison of corrosion rates between experimental and computed results from the model for mild steel at various combinations of variables as given in Table 3

concentration but the effect of pH is interesting. At lower Cl concentration, increase of alkalinity decreases the corrosion rate, while at higher Cl ion concentration, increase of pH enhances the corrosion rate. Alkalinity helps in formation of passive layer on stainless steel surface and so decrease of corrosion rate with increase in pH is justified at lower level of Cl ion concentration. At very high Cl ion concentration, fast rate of localized corrosion with anodic dissolution of metal takes place which enhances the rate of cathodic reaction at cathodic sites close to pitting areas and hence more generation of hydroxyl ions OH. With increase of pH, local alkalinity at sites near passive layer may become very high over 12.5, when

the oxide layer no more remains passive and so corrosion rate increases drastically.

The effects of sulfate (SO_4^{2-}) and chloride ion Cl^- concentration with pH 4 and 8 are shown in Fig. 4. Sulfate ion has a marginal effect in reducing the corrosion rate. The effect is more pronounced at higher pH 8. This may be due to the fact that presence of sulfate ion helps in formation of calcareous deposit which is favored with increase in alkalinity. With presence of Ca and Mg ions in the artificial seawater in the present investigation, the formation of calcareous deposit is assisted by SO_4^{2-} ions. The 3D surface of the corrosion rate (Fig. 4) at pH 4 is always higher than that at pH 8, but it is to be

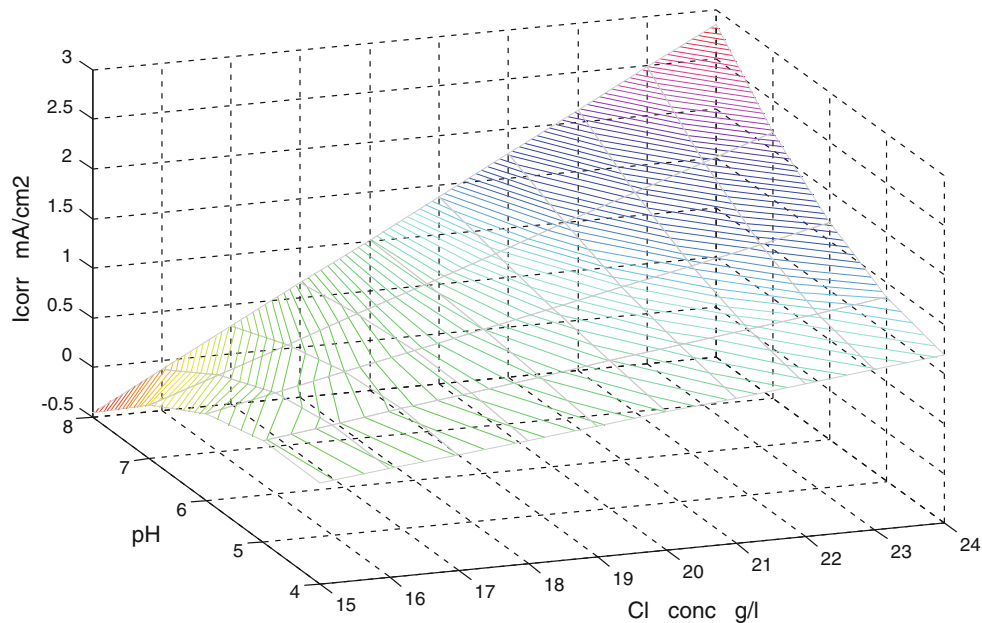


Fig. 3 Corrosion rate of 304 steel in artificial seawater as function of Cl concentration and pH

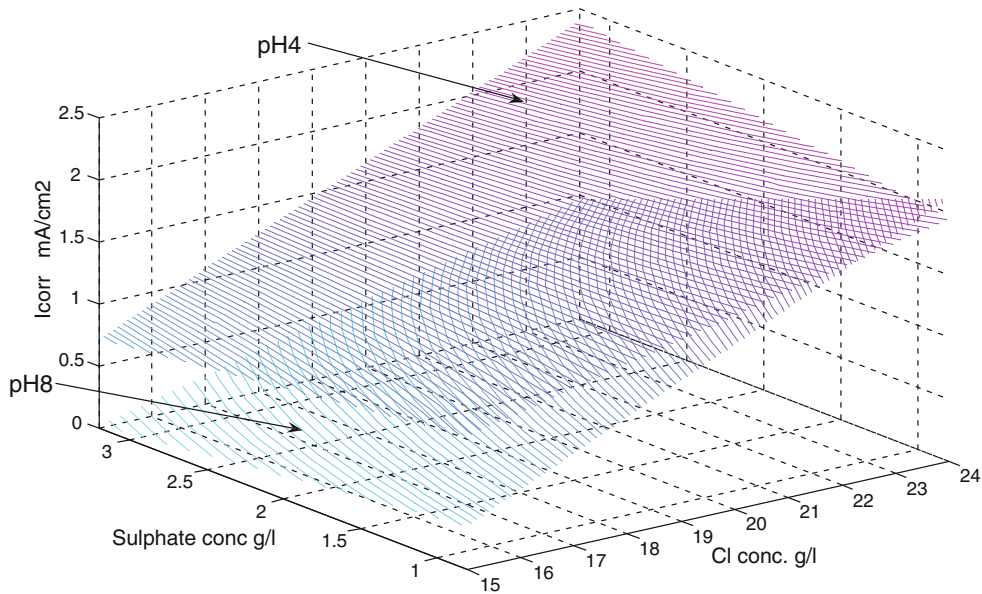


Fig. 4 Corrosion rate of 304 steel as function of sulfate and chloride concentration in artificial seawater at pH 4 and 8

noted that at higher Cl and lower SO_4^{2-} concentration the surface at pH 8 approaches that at pH 4 and overcomes it at highest level. This further supports the reasons, already explained in the previous paragraph, for drastic increase of corrosion rate at high pH with higher chloride level. Figure 5 displays two corrosion surfaces at lower and higher Cl content with variation of pH and sulfate ion. The ISO corrosion contour lines at lower surface is interesting, while at higher Cl content, it is almost linear. It is reflected from the lower surface that the conjoint effects of pH and sulfate, together have strong influence on corrosion rate. Formation of calcareous deposit with presence of sulfate ion is very much controlled by degree of acidity and alkalinity in the vicinity of corroding surface.

Three-dimensional mapping for the corrosion rate of mild steel as functions of pH and Cl content has been shown in Fig. 6. While the effect of Cl on the corrosion rate is simple linear, increasing with Cl content, that of sulfate and pH are inter-related and dependent on concentration of other parameters. Corrosion surface at lower sulfate concentration is at higher level at higher pH while it is the reverse at the lower pH. That is the SO_4^{2-} aggravates degradation of mild steel in acidic seawater, but it seems to help the formation of corrosion resistive deposit in alkaline seawater. The inter-relationship of pH and sulfate on corrosion rate is also reflected in Fig. 7, which shows the corrosion rate is maximum at an intermediate sulfate concentration and pH while the relation is linearly

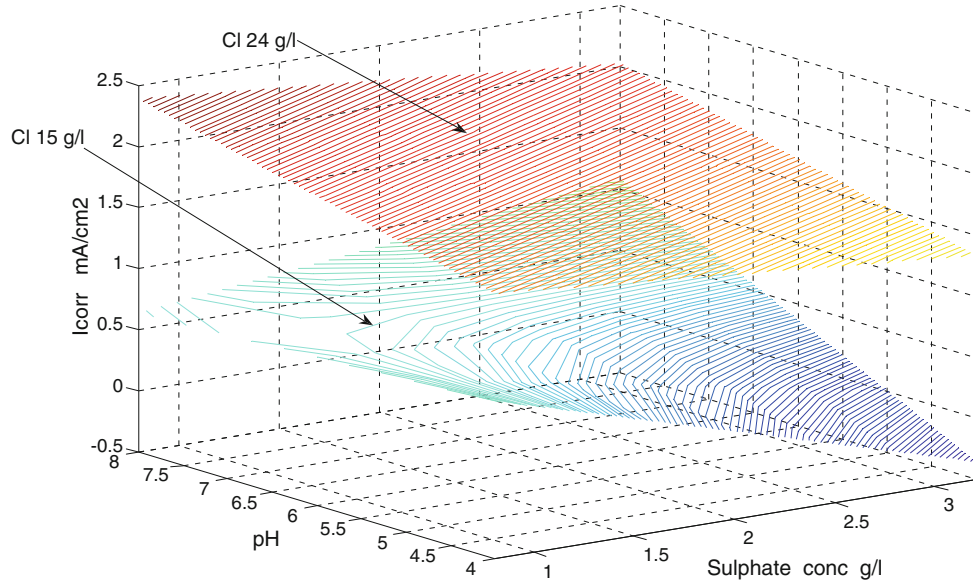


Fig. 5 Corrosion rate of 304 steel in artificial seawater as function of sulfate and pH at fixed Cl concentration

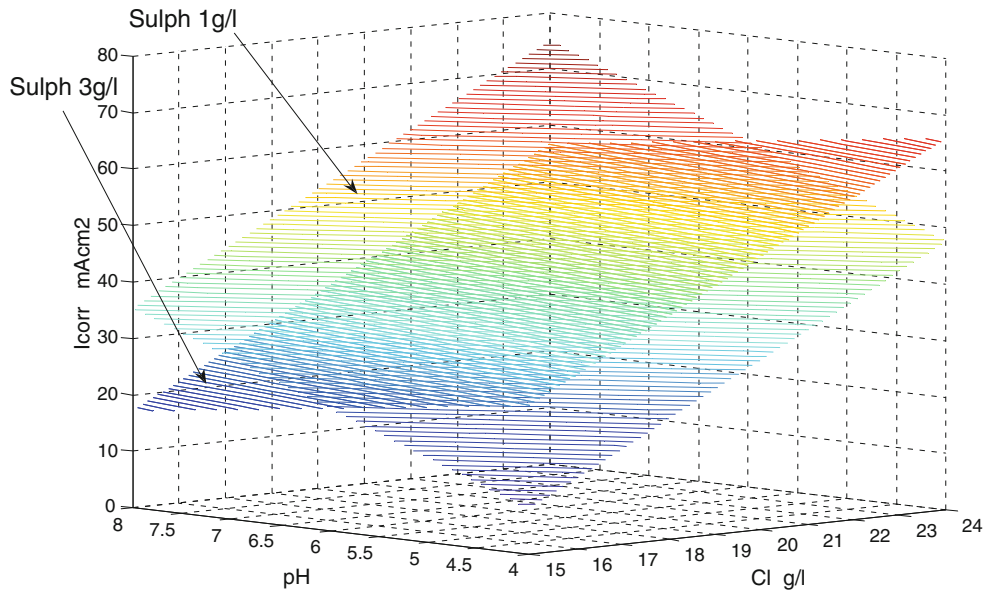


Fig. 6 Corrosion rate of mild steel in artificial seawater as function of pH and Cl at SO_4 ion concentration 1 and 3 g/L

increasing at lower pH and decreasing at higher pH. Figure 8 depicts the effects of temperature and Cl concentration at two fixed dissolved [O] concentration on the corrosion rate of mild steel. It is interesting to note that the effects of both temperature and Cl concentration which are known to enhance the degradation rapidly, have marginal effects on corrosion rate at 1 ppm concentration of dissolved [O]. It is also seen that the rate of increase of corrosion with the Cl concentration is very much influenced by temperature, that is, warmer the water, the higher the effect of Cl on I_{corr} and vice versa. It is due to the fact that temperature increases the mass transport of

Cl ion and decreases the concentration polarization. Figure 9 is another interesting figure which shows influence of [O] and Cl on the corrosion rate at lower temp 10 °C. Although it is known that the higher the Cl concentration or [O] concentration, the greater is the corrosion rate, it is seen here that it is giving minimum I_{corr} value at maximum Cl level when the [O] is also high and vice versa. That is, the single effect of any of them on corrosion is linearly increasing, but conjoint effect is complex and may decrease the rate. However, at higher temperature 40 °C, in Fig. 10, it is simple linear relationship as expected.

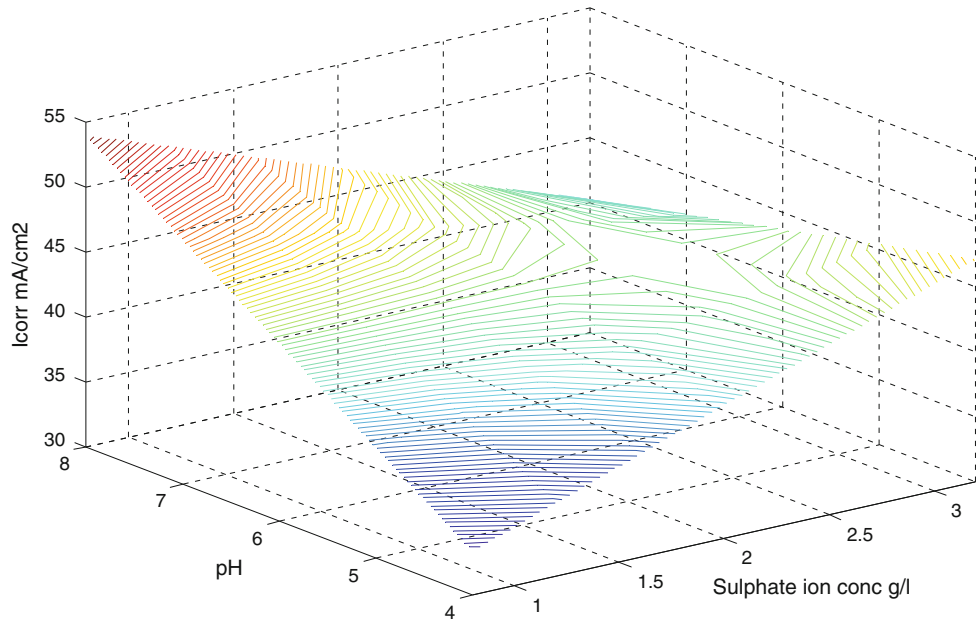


Fig. 7 Corrosion rate of mild steel in artificial seawater as a function of pH and sulfate ion concentration at 20 g/L chloride concentration

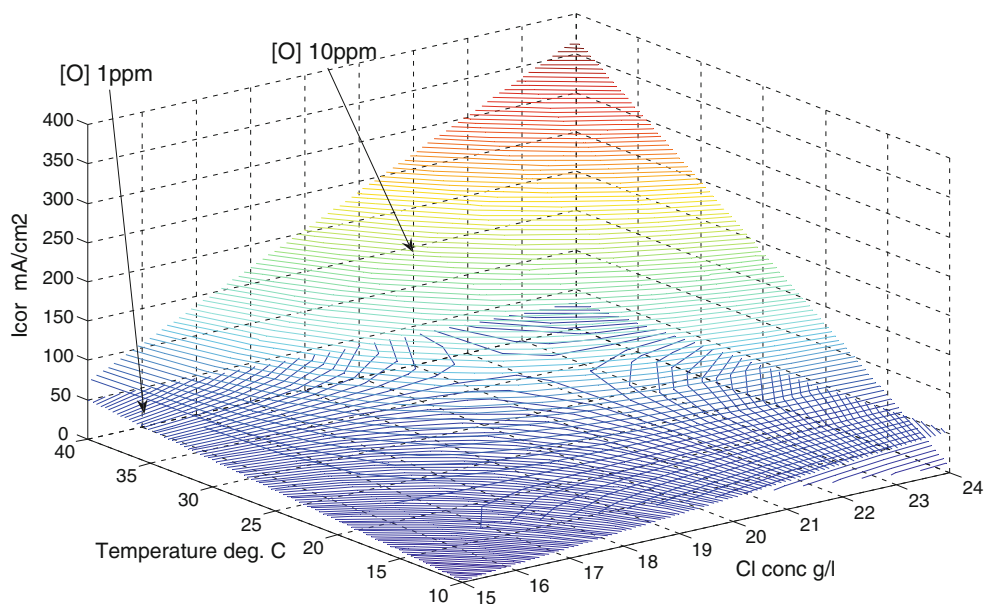


Fig. 8 Corrosion rate of mild steel in artificial seawater as a function of chloride concentration and temperature at 1.7 g/L sulfate ion concentration dissolved oxygen concentration 1 and 10 ppm

Figure 11 illustrates a comparison of 3D visual corrosion resistance behavior of mild steel and stainless steel with effect of Cl and SO_4^{2-} . In these figures (Fig. 1 and 12), I_{corr} values for 304 steel have been modified to 10 times I_{corr} ($10 \times I_{\text{corr}}$) while plotting, for better visualization and understanding of the comparative corrosion rates of two metals as the corrosion rates of 304 steel are too low compared to that of MS. It is seen that the effect of Cl concentration on corrosion rate is very sharp increase for the mild steel, compared to that of stainless steel. Effect of sulfate is also interesting, while for the MS,

the corrosion rate decreases with it, for 304, it increases marginally with SO_4^{2-} . Figure 12 is the similar diagram, showing effects of pH and SO_4^{2-} . Here it is also seen that the behavior of the materials are not similar with changes in pH or SO_4^{2-} . At lower pH, the presence of the SO_4^{2-} ions seems to help in reducing the corrosion rate of the stainless steel while it increases the rate for MS. At the other end of figure that is at higher pH, in neutral or little alkaline seawater, the effect is opposite. This reflects that the two steels do not behave in a similar way in aqueous marine environment.

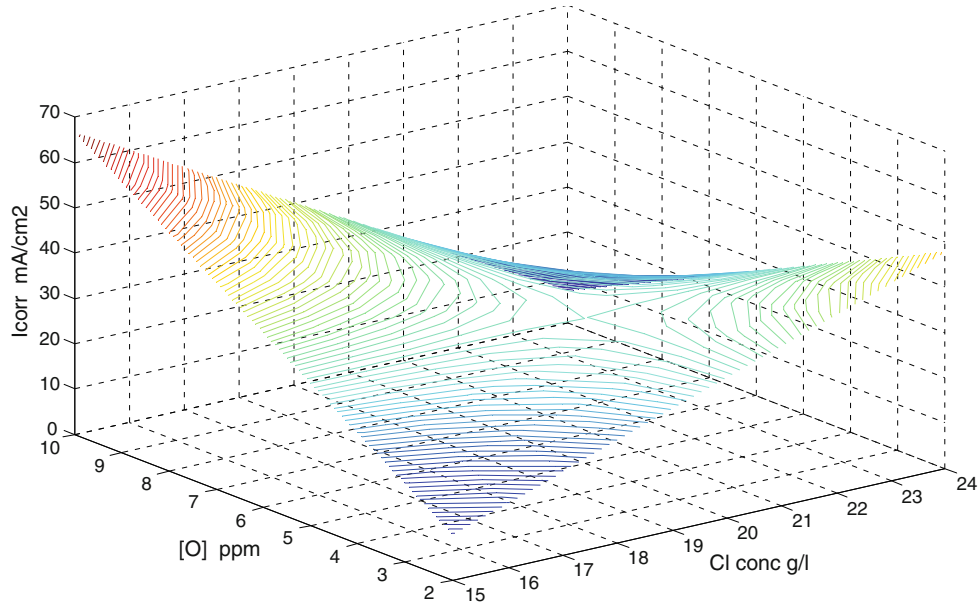


Fig. 9 Corrosion rate of mild steel in artificial seawater as a function of dissolved oxygen and chloride ion concentration at 1.7 g/L sulfate ion concentration at 10 °C

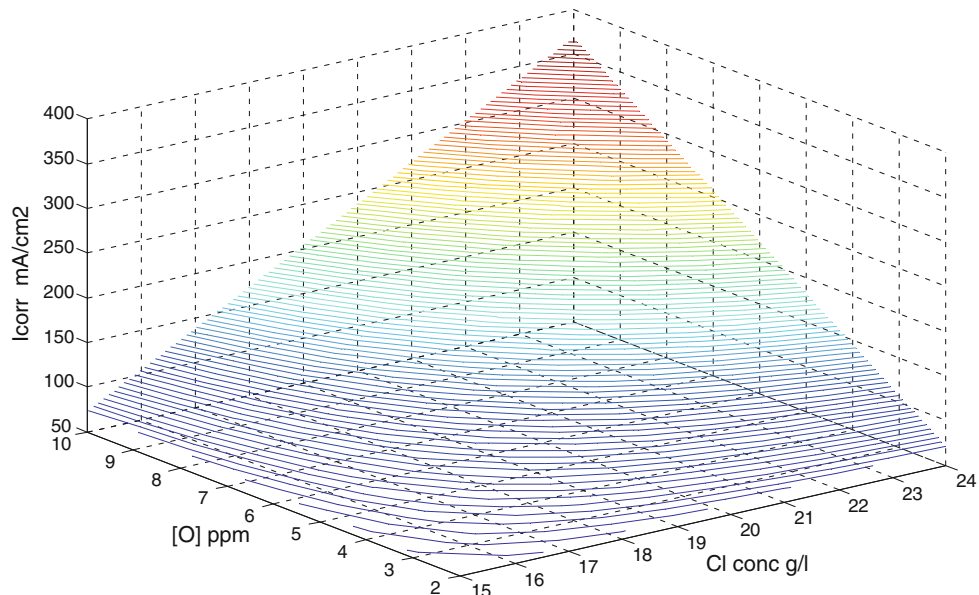


Fig. 10 Corrosion rate of mild steel in artificial seawater as a function of dissolved oxygen and chloride ion concentration at 1.7 g/L sulfate ion concentration at 40 °C

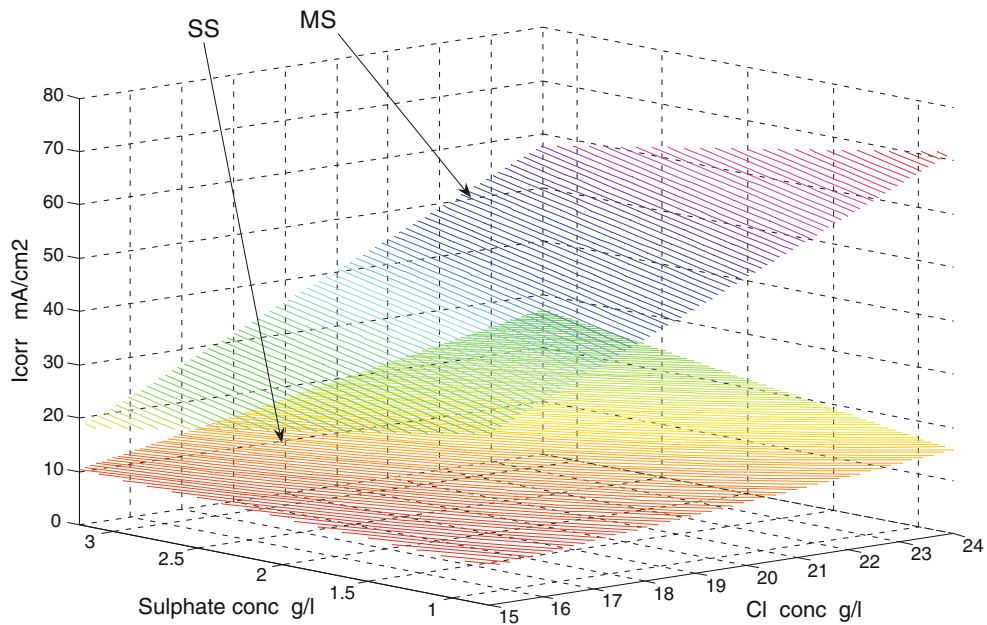


Fig. 11 Comparison of corrosion rate of mild steel with 304 steel in artificial seawater function of SO_4 and Cl concentration water

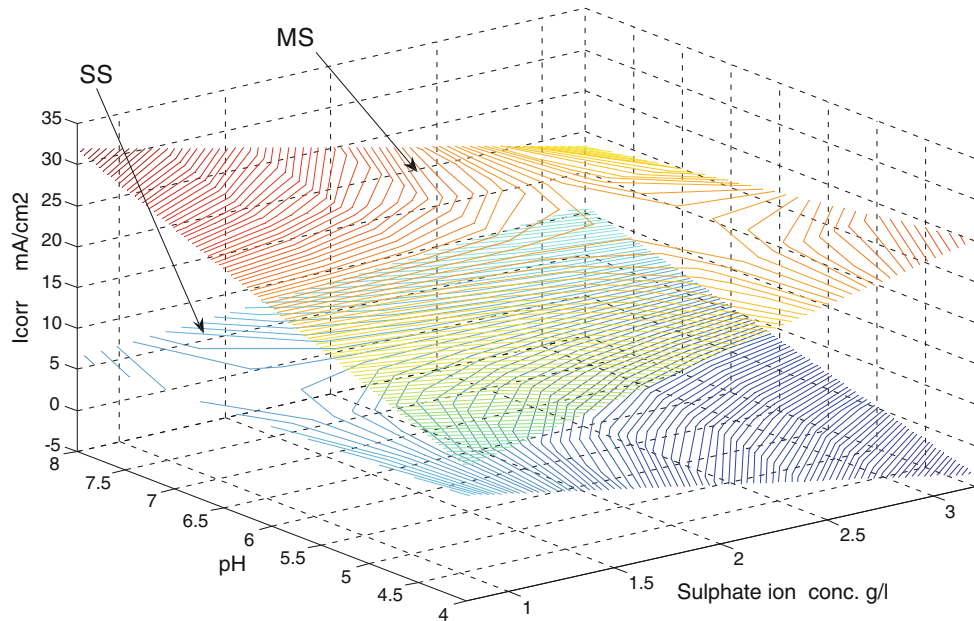
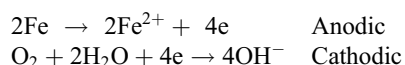


Fig. 12 Comparison of corrosion rate of mild steel and 304 steel in artificial seawater at 15 g/L Cl concentration with variation of pH and sulphate ion concentration

The electrochemical corrosion of carbon steel in aqueous environment like seawater takes place by the following anodic and cathodic reactions.



It is seen that the concentration of dissolved oxygen, O_2 , enhances the rate of cathodic reaction. It is known from the polarization diagram of the low carbon steel in aerated aqueous environment (Ref 16) that the anodic line cuts at concentration polarization region of the cathodic polarization curve at

$E_{corr} - I_{corr}$ point. The rate of cathodic reaction is controlled by I_L , the limiting current density, which is a strong function of concentration and diffusion of oxygen from the bulk solution to the interface. These explain the enhancement of corrosion rate with increase of dissolved oxygen concentration. The limiting current density is also very much influenced by the temperature and agitation, both of which increase with diffusion rate. Chloride ion increases the rate of first reaction (anodic) by forming metal chloride, which hydrolyzes to generate H^+ ions, increasing local acidity that aggravates further the dissolution process. It is also interesting to note the conjoint effects of pH

and sulfate (SO_4^{2-}) on the corrosion rate. The effect of temperature and dissolved oxygen ([O]) content on corrosion rate has also been found to support the electrochemical theory and polarization of steel in aqueous system (Ref 16).

8. Conclusion

The model developed is found to compute the corrosion rates which were close to experimental determined values within $\pm 10\%$ error. It can predict the corrosion rate and hence life of a submerged structure for a given geographical location in any ocean. Corrosion behavior of mild steel and 304 stainless in seawater can be visually studied from 3D mappings as functions of various combinations of concentration of Cl^- , SO_4^{2-} ions, pH, temperature, and dissolved [O]. The effects of these parameters are found to be not simple linear relation but interrelated and very much dependent on one another.

Appendix: Experimental Results

Table A1 Experimental data of corrosion rate of mild steel in artificial sea water with variation of water chemistry, pH, and temperature

Expt. no.	X1	X2	X3	X4	X5	Z
1	15	4	0.8	25	6	22.2725
2	15	4.8	0.8	25	6	22.0325
3	15	5.6	0.8	25	6	21.7925
4	15	6.4	0.8	25	6	21.5525
5	15	7.2	0.8	25	6	21.3125
6	15	8	0.8	25	6	21.0725
7	15	4	0.8	25	6	22.2725
8	15	4	1.32	25	6	21.5135
9	15	4	1.84	25	6	20.7545
10	15	4	2.36	25	6	19.9955
11	15	4	2.88	25	6	19.2365
12	15	4	3.4	25	6	18.4775
13	15	4	3.92	25	6	17.7185
14	15	4	0.8	25	6	22.2725
15	16.8	4	0.8	25	6	28.1405
16	18.6	4	0.8	25	6	34.0085
17	20.4	4	0.8	25	6	39.8765
18	22.2	4	0.8	25	6	45.7445
19	24	4	0.8	25	6	51.6125
20	25.8	4	0.8	25	6	57.4805
21	24	8	3.4	25	6	37.5275
22	24	7.2	3.4	25	6	47.0395
23	24	6.4	3.4	25	6	56.5515
24	24	5.6	3.4	25	6	66.0635
25	24	4.8	3.4	25	6	75.5755
26	24	4	3.4	25	6	85.0875
27	24	8	3.4	25	6	37.5275
28	24	8	2.88	25	6	44.2225
29	24	8	2.36	25	6	50.9175
30	24	8	1.84	25	6	57.6125
31	24	8	1.32	25	6	64.3075
32	24	8	0.8	25	6	71.0025
33	24	8	0.28	25	6	77.6975
34	24	8	3.4	25	6	37.5275
35	22.2	8	3.4	25	6	34.9955

Table A1 Continued

Expt. no.	X1	X2	X3	X4	X5	Z
36		20.4	8	3.4	25	6
37		18.6	8	3.4	25	6
38		16.8	8	3.4	25	6
39		15	8	3.4	25	6
40		13.2	8	3.4	25	6
41		15	8	2.1	10	2
42		15	8	2.1	10	3.6
43		15	8	2.1	10	5.2
44		15	8	2.1	10	6.8
45		15	8	2.1	10	8.4
46		15	8	2.1	10	10
47		15	8	2.1	10	11.6
48		15	8	2.1	10	2
49		15	8	2.1	16	2
50		15	8	2.1	22	2
51		15	8	2.1	28	2
52		15	8	2.1	34	2
53		15	8	2.1	40	2
54		15	8	2.1	40	2
55		15	8	2.1	10	2
56		16.8	8	2.1	10	2
57		18.6	8	2.1	10	2
58		20.4	8	2.1	10	2
59		22.2	8	2.1	10	2
60		24	8	2.1	10	2
61		25.8	8	2.1	10	2
62		24	8	2.1	40	10
63		24	8	2.1	40	8.4
64		24	8	2.1	40	6.8
65		24	8	2.1	40	5.2
66		24	8	2.1	40	3.6
67		24	8	2.1	40	2
68		24	8	2.1	40	10
69		24	8	2.1	34	10
70		24	8	2.1	28	10
71		24	8	2.1	22	10
72		24	8	2.1	16	10
73		24	8	2.1	10	10
74		24	8	2.1	40	10
75		22.2	8	2.1	40	10
76		20.4	8	2.1	40	10
77		18.6	8	2.1	40	10
78		16.8	8	2.1	40	10
79		15	8	2.1	40	10
80		13.2	8	2.1	40	10
81		19.5	6	3.1	25	6
82		19.5	6	3.1	25	6
83		19.5	6	3.1	25	6
84		19.5	6	2.1	25	6
85		19.5	6	2.1	25	6
86		19.5	6	2.1	25	6
87		17	7	3	13	5

X1 = Cl concentration, g/L; X2 = pH; X3 = SO_4 concentration, g/L; X4 = temperature, $^{\circ}\text{C}$; X5 = Dissolved [O] concentration, ppm; Z = corr rate, $\mu\text{A}/\text{cm}^2$

References

1. Dechema Handbook of Corrosion, Vol. 11, VCH Publishers, Weinheim, NY, 1992, p 66
2. U.R. Evans, *The corrosion and Oxidation of Metals: Scientific Principles and Practical Applications*, Edward Arnold (Publishers) Ltd., London, 1960

3. R.E. Melchers and R. Jeffrey, Influence of Water Velocity on Marine Corrosion of Mild Steel, *Corrosion (NACE)*, 2004, **60**, p 84–94
4. L.A. Terry and R.G.J. Edyvean, Influences of Microalgae on Corrosion of Structural Steel, *Corrosion and Marine Growth on Offshore Structures*, J.R. Lewis and A.D. Mercer, Ed., 1984, p 38–44
5. B.D. Craig, *Handbook of Corrosion Data*, ASM International, OH, 1989
6. N. Sridhar, C.S. Brossia, D. S. Dunn, and A. Anderko, Predicting Localized Corrosion in Seawater, *Corrosion (NACE)*, 2005, p 915
7. R.E. Melchers, Effect of Temperature on the Marine Immersion of Corrosion of Carbon steels, *Corrosion (NACE)*, 2002, p 762
8. M.L. Free, Tri Service, *Corrosion Conference*, 2005, p 1
9. M.L. Free, W. Wang, and D.Y. Ryu, Prediction of Corrosion Inhibition Using Surfactants, *Corrosion*, 2004, **60**, p 837
10. J.R. Scully, Polarization Resistance Method for Determination of Instantaneous Corrosion Rates, *Corrosion*, 2000, **56**, p 199
11. ASTM G 5: Potentiostatic and Potentiodynamic Anodic Polarization Measurements
12. ASTM G 59: Polarization Resistance Measurements
13. ASTM G 61: Cyclic Polarization Measurements for Localized Corrosion
14. N.G. Thompson and J.H. Payer, *DC Electrochemical Test Methods*, National Association of Corrosion Engineers, 1440 South Creek Drive, Houston, TX 77084-4906
15. C. Douglas, *Montgomery, Design and Analysis of Experiments*, 2nd ed., Wiley and Sons, New York, NY, 1988
16. D.A. Jones, *Principles and Prevention of Corrosion*, 2nd ed., Prentice Hall, London, 1996, p 92